IEICE TRANS. COMMUN., VOL.E104–B, NO.10 OCTOBER 2021

PAPER Special Section on Dynamic Spectrum Sharing for Future Wireless Systems

A Spectrum Regeneration and Demodulation Method for Multiple Direct Undersampled Real Signals

Takashi SHIBA[†a)], ***Member***, **Tomoyuki FURUICHI**[†], ***Student Member***, **Mizuki MOTOYOSHI**[†], ***Member***, **Suguru KAMEDA**[†], ***Senior Member***, ***and*** **Noriharu SUEMATSU**[†], ***Fellow***

SUMMARY We propose a spectrum regeneration and demodulation method for multiple direct RF undersampled real signals by using a new algorithm. Many methods have been proposed to regenerate the RF spectrum by using undersampling because of its simple circuit architecture. However, it is difficult to regenerate the spectrum from a real signal that has a band wider than a half of the sampling frequency, because it is difficult to include complex conjugate relation of the folded spectrum into the linear algebraic equation in this case. We propose a new spectrum regeneration method from direct undersampled real signals that uses multiple clocks and an extended algorithm considering the complex conjugate relation. Simulations are used to verify the potential of this method. The validity of the proposed method is verified by using the simulation data and the measured data. We also apply this algorithm to the demodulation system.

key words: *direct undersampling, real signal, sub-nyquist, spectrum regeneration, compressed sensing, IoT, demodulation*

1. Introduction

Recently, the market of the Internet of Things (IoT) [1] has become wider as is well known. The communication systems of IoT applications are almost wireless systems because the arrangement of equipments in the industry changes frequently. The cognitive wireless system [2], [3] using software-radio is a promising technology for IoT. One wireless frequency channel is used in a vacant band by searching a vacant spectrum band in this case. A spectrum monitor is necessary for this kind of system. Many spectrum regeneration methods [4]–[25] have been studied that use analog to digital converters (ADCs) for this kind of monitor as shown in Table 1. The fundamental solution is the direct Nyquist sampling method because of its simple architecture. However, a high-speed sampling ADC is necessary for the wideband signal. Many signal mixing applications [4]–[15] are studied for this problem. This method is a useful solution except for the disadvantage of some additional mixers and some local oscillators. Direct undersampling technology is also useful with a low sampling rate and a simple circuit architecture. The special spectrum regeneration method is necessary in this case. Some direct undersampling methods to regenerate the RF spectrum are proposed. The selected sampling frequency method [16] is useful when RF bandwidth is narrow. However, RF bandwidth has a wide-range in almost any case. Multiple coset phase sampling method [17], [18] is useful for wideband signal, however, the precise control for different phase is necessary. Multiple sampling frequency method [19]–[21] is useful for a wideband signal if the sampled signals after ADC are treated as real. However, the sampled signals are treated as a complex signal or simple signal ignoring spectrum folding in these conventional cases. We need to set IQ-baseband-mixer with the circuit complexity in order to obtain these complex signals. Power spectrum estimation methods [22]–[25] are useful when only power (not complex) spectrums are required.

We propose a direct undersampling method treating real signals after multiple ADCs to regenerate the wider band complex spectrum than the half of Nyquist frequency without any mixer. The direct undersampling signals should be treated as real sampled signals. There are three problems in this case.

(1) There are both forward and backward frequency directions for even and odd folding spectrums.
(2) Each even and odd folded spectrum element of the same RF frequency has a relation to the complex conjugate.
(3) Folded spectrum element has a convolution value of these two complex conjugate elements at wrap frequency.

Generally, it is difficult to include the complex conjugate transformation in the general linear algebraic equation. Therefore, it is difficult to make an algorithm in the former real signal case because the condition includes a complex conjugate relation. We propose a new reconstruction method by using an extended algorithm based on the compress sensing [26] including a relation of a complex conjugate, a folding direction for folded spectrums and a convolution of even/odd spectrums at wrap frequency. We apply this technique for wireless IoT band to verify the effectiveness of this method using simulation and measured data. We also apply this technique to a demodulation system in order to confirm feasibility of software tunable function without IF or baseband filter or high frequency ADC.

2. Spectrum Regeneration Method

A proposed spectrum regeneration system using multiple clocks (sampling frequency fs) undersampling ADC is shown in Fig. 1. We apply the Fast Fourier Transform (FFT) for the multiple real signals in order to transform to undersampled complex spectrums. We will explain our ideas at first. We consider the simple condition of original spectrums

Manuscript received November 2, 2020.
Manuscript revised February 20, 2021.
Manuscript publicized March 30, 2021.

[†]The authors are with Research Institute of Electrical Communication, Tohoku University, Sendai-shi, 980-8577 Japan.
a) E-mail: shiba@riec.tohoku.ac.jp

DOI: 10.1587/transcom.2020DSP0006

Table 1 Comparison of spectrum regeneration system.

Spectrum regenerating method	Direct sampling	Direct undersampling						Signal mixing
	Nyquist sampling	Selected frequency sampling	Multiple coset phase sampling	Multiple frequency sampling	Spectrum sequential solution	Spectrum and-process	This work	Xampling etc.
Wider regenerated bandwidth than half sampling maximum frequency	no	no	possible	possible	possible	yes	yes	possible
N. of ADC	1	multiple	multiple	multiple	multiple (2)	1	multiple	multiple
N. of sampling rate	1	multiple	1	multiple	multiple (2)	multiple	multiple	1
N. of sampling phase	1	1	multiple	1	1	1	1	1
different phase setting	no	no	need precise different phase setting	no	no	no	no	no
Treating type of signal after ADC	real	real	real	as complex	real	real	real	complex
Type of regenerated spectrum elements	complex	real (power)	complex	complex	real (power)	real (power)	complex	complex
Considering Even/Odd spectrum folding and complex-conjugate relation	no need	no need	no need	no	no need	no need	yes	no need
References	-	[16]	[17] [18]	[19]-[21]	[22]-[24]	[25]	-	[4]-[15]

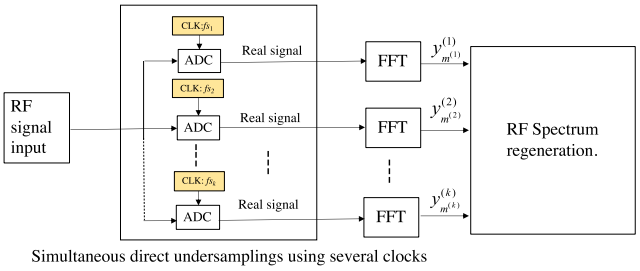

Fig. 1 Frequency spectrum regeneration system.

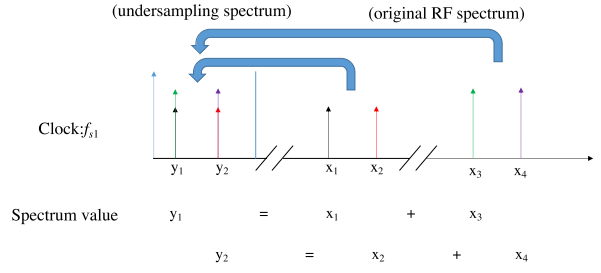

Fig. 2 Relation between undersampling spectrums and original RF spectrums.

and undersampling spectrums as shown in Fig. 2. A relation between original RF complex spectrums x_1, x_2, x_3, x_4 and undersampling spectrums y_1, y_2 are expressed by simple equations,

$$\begin{pmatrix} y_1 \\ y_2 \end{pmatrix} = \begin{pmatrix} x_1 + x_3 \\ x_2 + x_4 \end{pmatrix}. \tag{1}$$

This equation can be expressed by using equation,

$$\begin{pmatrix} y_1 \\ y_2 \end{pmatrix} = \begin{pmatrix} 1x_1 + 0x_2 + 1x_3 + 0x_4 \\ 0x_1 + 1x_2 + 0x_3 + 1x_4 \end{pmatrix} = \begin{pmatrix} 1 & 0 & 1 & 0 \\ 0 & 1 & 0 & 1 \end{pmatrix} \begin{pmatrix} x_1 & x_2 & x_3 & x_4 \end{pmatrix}. \tag{2}$$

We define a desired frequency spectrum vector (x), a measured undersampled frequency spectrum vector (y) and a sparse coefficient matrix (A)

$$(y) = \begin{pmatrix} y_1 \\ y_2 \end{pmatrix}, \quad (x) = \begin{pmatrix} x_1 & x_2 & x_3 & x_4 \end{pmatrix},$$
$$(A) = \begin{pmatrix} 1 & 0 & 1 & 0 \\ 0 & 1 & 0 & 1 \end{pmatrix}, \tag{3}$$

we can obtain a linear algebraic equation,

$$(y) = (A)(x). \tag{4}$$

We expand n-th order (x) and m-th order (y). Even if n is higher than m, we can obtain a sparse solution by the compressed sensing algorithm [26]. It is important how to treat folded spectrums in this real undersampled signal case. We adjust a total sampling time Tt for each kth clock ADC so that a spectrum frequency resolution

$$\Delta f = \frac{1}{Tt} = \frac{fs_k}{Ns_k}, \tag{5}$$

become a constant. Here fs_k is sampling frequency and Ns_k is the number of sampling points of k-th ADC respectively. We transform each frequency f to digitized value

$$f\_d = \frac{f}{\Delta f}, \tag{6}$$

to set digitized frequencies corresponding to (x) and (y) vector to the same grids. Partial (x) vector is defined as

$$\left(x^{(l)}_{n^{(l)}}\right) = \left(x^{(l)}_1, x^{(l)}_2, \cdots, x^{(l)}_{2n^{(l)}-1}, x^{(l)}_{2n^{(l)}}, \cdots, x^{(l)}_{2N^{(l)}-1}, x^{(l)}_{2N^{(l)}}\right), \tag{7}$$

and there are $N^{(l)}$ elements for band l. Each element is a complex value corresponding to digitized frequency vector

$$\left(fx\_d_{n^{(l)}}^{(l)}\right)=\left(fx\_d_{1}^{(l)}, fx\_d_{1}^{(l)}, \cdots, fx\_d_{N^{(l)}}^{(l)}, fx\_d_{N^{(l)}}^{(l)}\right). \quad (8)$$

Here, each element $x_{m^{(l)}}^{(l)}$ are paired as

$$x_{2q-1}^{(l)} = \overline{x_{2q}^{(l)}} \quad (2q \le N^{(l)}, q\text{: } nature\ number), \quad (9)$$

corresponding to a folding number Q which is defined by

$$Q = \lfloor (fx\_d_n) / (Ns_k/2) \rfloor . \quad (10)$$

An element of $x_{2q-1}^{(l)}$ is corresponding to Q=zero or even number of a folded spectrum and an element of $x_{2q}^{(l)}$ is corresponding to Q=odd number of folded spectrum. We set the complex conjugated pair elements for Q=odd or even number to the neighbor elements of (x). A partial (y) vector is defined as regeneration from undersampling by using compressed sensing method.

$$\left(y_{m^{(k)}}^{(k)}\right) = \left(y_{1}^{(k)}, y_{2}^{(k)}, \cdots, y_{m^{(k)}}^{(k)}, \cdots, y_{M^{(k)}}^{(k)}\right)^T, \quad (11)$$

for a measured spectrum by k-th clock undersampling ADC. The number of $y_{m^{(k)}}^{(k)}$ is $M(k)$. A digitized frequency vector corresponding to $\left(y_{m^{(k)}}^{(k)}\right)$ is also defined as

$$\left(fy\_d_{m^{(k)}}^{(k)}\right) = \left(0, 1, \cdots, fy\_d_{m^{(k)}}^{(k)}, \cdots, fy\_d_{M^{(k)}}^{(k)} = Ns_k/2\right)^T \quad (12)$$

We make total (x) and (y) connecting partial (x) and (y) vectors. We also make a maximum digitized frequency vector $(fy\_d\_\max_m)$ as

$$\left(fy\_d\_\max_m\right) = \{(Ns_1/2, \cdots, Ns_1/2), \cdots, (Ns_k/2, \cdots, Ns_k/2)\}. \quad (13)$$

We set each element of (A) to 1 when folded frequency corresponding to (x) is the same as the frequency corresponding to (y). An example relation between the original RF spectrum and the undersampled spectrum transformed by FFT from the real signal of clock 1 ADC is shown in Fig. 3. Element value (1 or 0) of (A) is decided by Q. If Q corresponding to Band:1 frequency is even, we set 1 for a coefficient of $x_{2n^{(1)}-1}^{(1)}$ and If Q corresponding to Band:2 frequency is odd, we set 1 for a coefficient of $x_{2n^{(2)}}^{(2)}$. Frequency directions between undersampled and original spectrum are opposite for Band:2 (Q=odd number) in this case. The second example for clock 2 at a wrap frequency is shown in Fig. 4. We show a special example that the target frequency is wrap frequency at boundary even and odd Q areas. We set 1 for the both even and odd elements of (A) corresponding to coefficients of $x_{2n^{(1)}-1}^{(1)}$, $x_{2n^{(1)}}^{(1)}$ and $x_{2n^{(2)}}^{(2)}$, $x_{2n^{(2)}-1}^{(2)}$.

We also define a sub-number vector (Tr) corresponding to each measured sampling frequency step for (y) as

$$(Tr_m) = \left\{\left(1, \cdots, M^{(1)} = Ns_1/2+1\right), \cdots, \left(1, \cdots, M^{(K)} = Ns_k/2+1\right)\right\}^T, \quad (14)$$

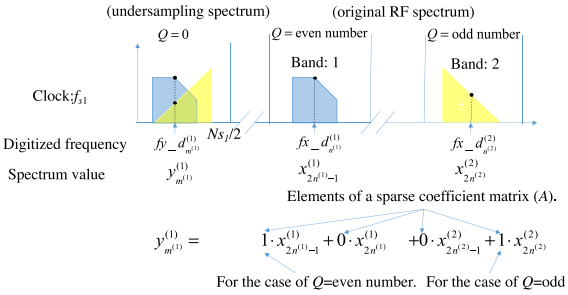

Fig. 3 Relation between the original RF and undersampling spectrum transformed from real signals.

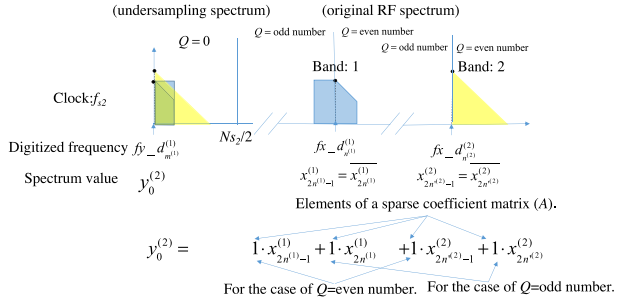

Fig. 4 Relation between the original RF and undersampling spectrum at wrap frequency transformed from real signals.

in order to make (A). We define each element of (A) as

$$A_{m,n} = \begin{cases} 1 & at\ condition\ B \\ 0 & others \end{cases}, \quad (15)$$

condition B
when $(Q = 0$ *or even number*$)$ *and* $(m =$ *odd number*$)$
$\quad$ *and* $Tr_m = R + 1$,
or
when $(Q =$ *odd number*$)$ *and* $(m =$ *even number*$)$
$\quad$ *and* $Tr_m = fy\_d\_max_m + 1 - R$,
or
when $(Q = 0$ *or even number*$)$ *and* $(m =$ *even number*$)$
$\quad$ *and* $R = 0$ *and* $Tr_m = 1$,
or
when $(Q =$ *odd number*$)$ *and* $(m =$ *odd number*$)$
$\quad$ *and* $R = 0$ *and* $Tr_m = fy\_d\_max_m + 1$. $\quad (16)$

Here,

$$R = fx\_d_n \bmod fy\_d\_max_m (= Ns_k/2). \quad (17)$$

An example about (A) setting with explain is shown in Fig. 5. We have prepared all parameters to apply an extended compressed sensing algorithm and to reconstruct spectrums. We use the Alternating Direction Method of Multipliers (ADMM) for the compressed sensing adding the routine

$$x_{2q-1} \to \left(x_{2q-1} + \overline{x_{2q}}\right)/2$$
$$x_{2q} \to \left(x_{2q} + \overline{x_{2q-1}}\right)/2, \quad (18)$$

to equalize even and odd folded spectrums from the direct

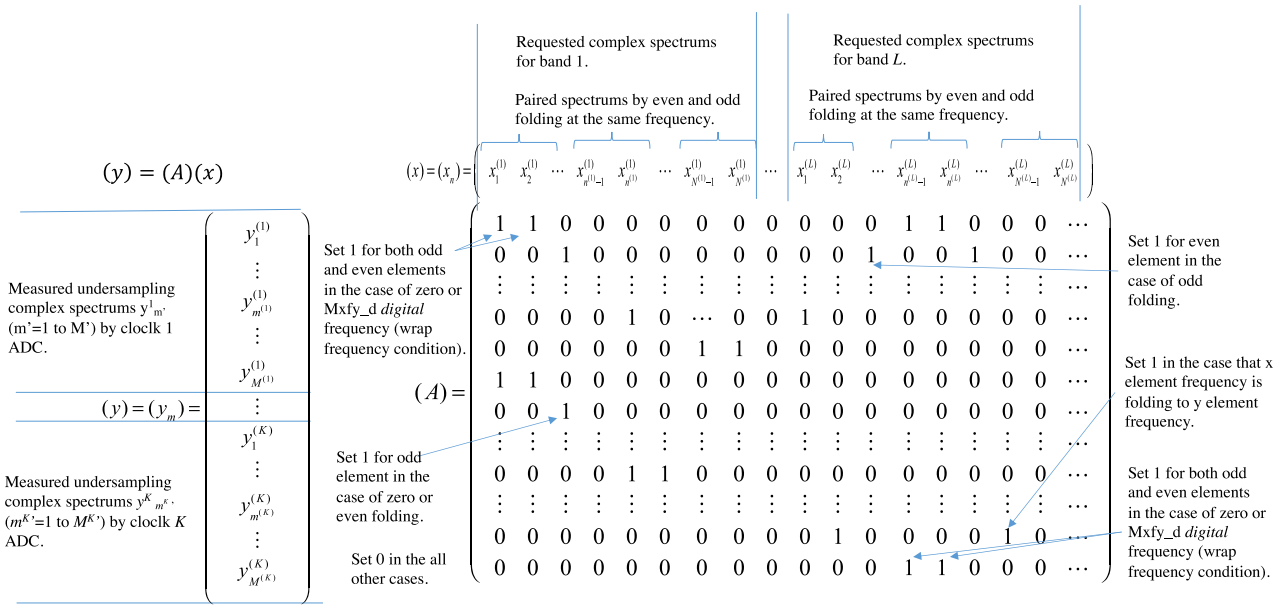

Fig. 5 Procedure how to make (x), (y) vector and (A) matrix for spectrum.

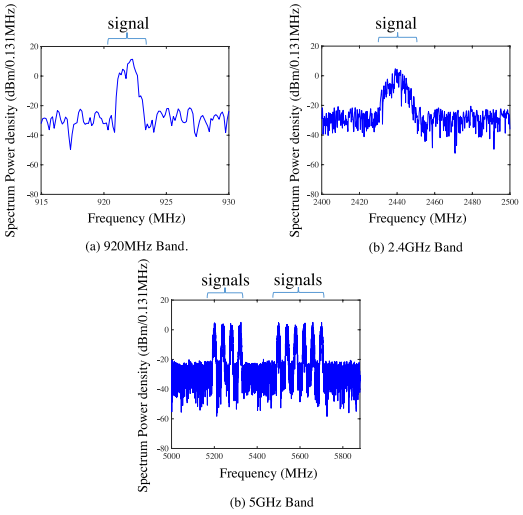

Fig. 6 Original RF spectrums for simulation.

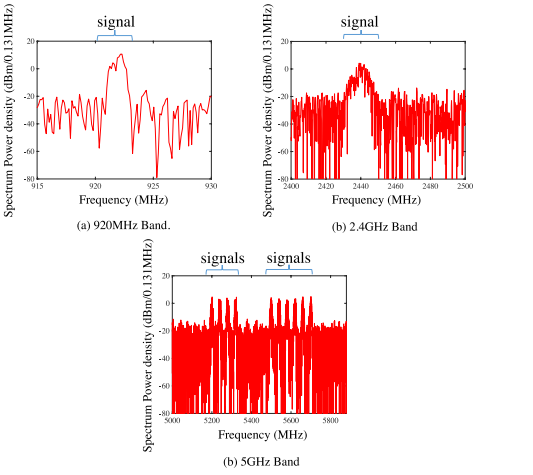

Fig. 7 Reconstruction spectrums by using the proposed method.

undersampled real signal.

3. Simulation for Verifying Proposed Method

We apply our proposed method to wireless IoT example. We use three ADCs and the parameters are
(a) $Ns_1 = 3822$, $fs1 = 500$ MHz, (b) $Ns_2 = 3136$, $fs_2 = fs_1 Ns_2/Ns_1$,
(c) $Ns3 = 2496$, $fs_3 = fs_1 Ns_3/Ns_1$
Then sampling time Tt becomes 7.644 µs for all ADCs. Three wireless IoT bands (Band1: 920 MHz Band, Band2: 2.4 GHz Band, Band3: 5 GHz Band) are set for example. We add white noise (condition: NF (noise figure) = 5 dB, $Gain$ (system gain) = 70 dB). Original spectrums are shown in Fig. 6. Regenerated spectrums are shown in Fig. 7. The regenerated spectrums are in good agreements with the original spectrums. We consider succeeding in the regeneration of spectrums.

4. Example Using Wireless IOT Measurement Data

We use some measured data of three desired wireless IoT bands for a signal source to verify the availability of the proposed method by using simulation. Measurement system for actual wireless IoT examples of RFID (920 MHz band), Bluetooth (2.4 GHz band) and Wireless LAN (5 GHz band) signals are shown in Fig. 8. We use a wideband antenna to obtain three (RFID, Bluetooth, Wireless LAN) mixed signals. A total system block for this evaluation is shown in Fig. 9. We need digital data for our algorithm simulation. We convert from an analog signal to digital high-speed sampling data by using an 80 GHz sampling oscilloscope. Un-

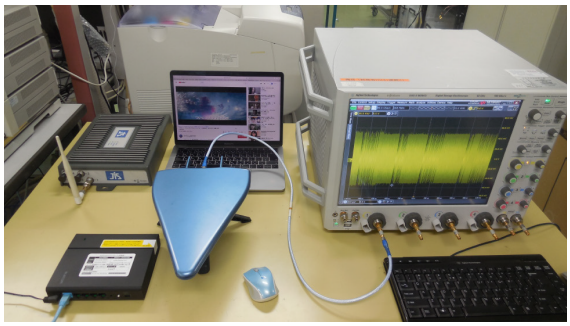

Fig. 8 Measurement system for RFID (920 MHz band), Bluetooth (2.4 GHz band) and Wireless LAN (5 GHz band).

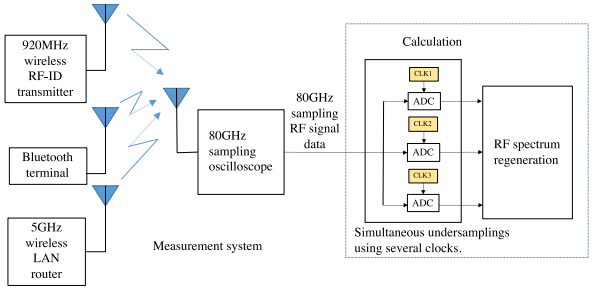

Fig. 9 Measurement and spectrum-regeneration system without a triplexer bandpass filter for RFID (920 MHz band), Bluetooth (2.4 GHz band) and Wireless LAN (5 GHz band).

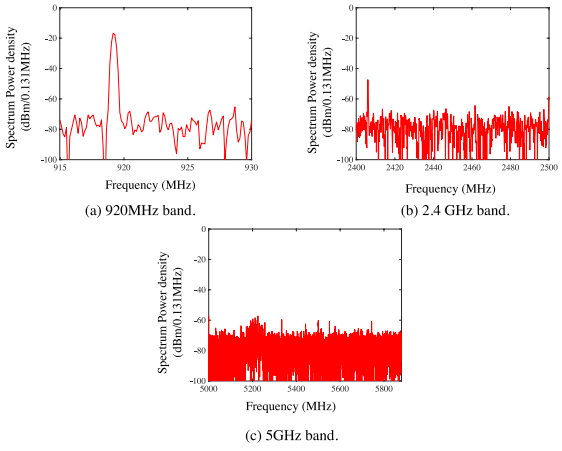

Fig. 10 Regenerated spectrum power density results for RFID (920 MHz band), Bluetooth (2.4 GHz band) and Wireless LAN (5 GHz band) measured signals from undersampling spectrum by using the proposed method without a triplexer bandpass filter.

dersampling signals are made from these data by using interpolation and we apply FFT to these undersampling real signals. We apply the same ADC condition as chapter 3 and the proposed algorithm of Sect. 2 to the FFT data and we can obtain a regenerated spectrum. Obtained results of spectrums are shown in Fig. 10. Characteristics of the peak to sidelobe ratios are relatively low because of noise-aliasing. Especially peaks to sidelobes for 5 GHz is lower. Results of *Peak* (peak level)/*U* (maximum sidelobe level): 10 dB and

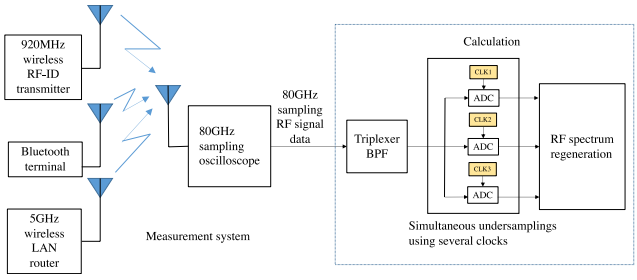

Fig. 11 Measurement and spectrum-regeneration system with a triplexer bandpass filter for RFID (920 MHz band), Bluetooth (2.4 GHz band) and Wireless LAN (5 GHz band).

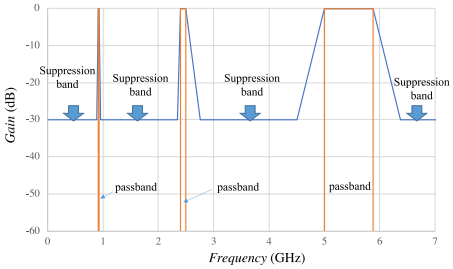

Fig. 12 Frequency characteristics of a triplexer bandpass filter using spectrum-regeneration system.

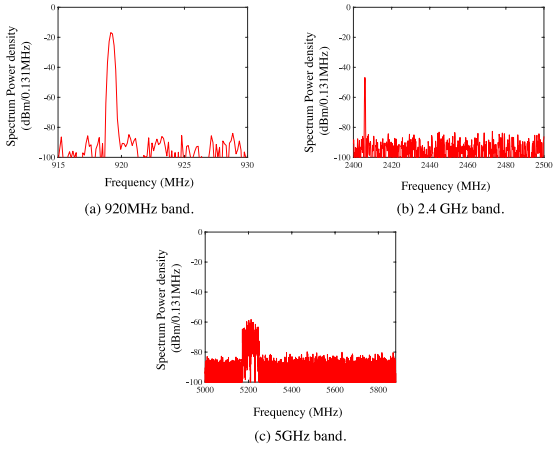

Fig. 13 Regenerated spectrum power density results for RFID (920 MHz band), Bluetooth (2.4 GHz band) and Wireless LAN (5 GHz band) measured signals from undersampling spectrum by using the proposed method with a triplexer bandpass filter.

Peak/*Uave* (average sidelobe level): 18 dB for 5 GHz band are obtained. This peak to sidelobe ratio is almost decided from peak and noise level. We consider that this peak to sidelobe is not enough for IoT spectrum control system and demodulation system.

Therefore, we set a filter before ADCs to suppress aliasing noise as shown in Fig. 11. Obtained measurement data are filtered by a triple bandpass filter (triplexer BPF) which characteristics are shown in Fig. 12, to suppress aliasing noise. We apply our spectrum regeneration method to this spectrum. Each obtained spectrum for desired bands 1 to 3 is shown in Fig. 13. Each RF spectrums are obtained

by the regeneration process. Results of *Peak*/*U*: 23 dB and *Peak*/*Uave*: 33 dB for 5GHz band are obtained. We consider that the peak sidelobe ratio is sufficient for IoT spectrum control system and demodulation system, because these values are over than 14 dB and sufficient 10^{-4} bit error rate is obtained at S/N 14 dB for QPSK example at our simulation of chapter 5. 10^{-4} bit error rate can become almost error-free by using error-collection method. We consider that we can succeed to regenerate spectrum in this case when using measured data.

5. Simulation Example of Demodulation

The regenerated frequency spectrum by using this proposed method has complex information. Therefore, we can select frequency and band, and we can obtain demodulated data by software from these complex spectrums. An advantage of this demodulation method is that the perfectly tunable function of a receiver can be obtained only using low frequency sampling ADCs and a top filter without IF and baseband filters. A demodulation system from an undersampled signal by using this proposed algorithm is shown in Fig. 14. The conditions of ADCs are the same as chapter 3. A mixing carrier $Smix(t)$ is expressed as

$$Smix(t) = e^{j\{-2\pi(fo-df)t+dphase\}}. \quad (19)$$

Here fo is a RF signal carrier frequency and df is a frequency compensation value and *dphase* is a phase compensation value, respectively. An aim of this chapter study is only to evaluate a demodulation function of the proposed method, therefore we select simple BPSK and QPSK modulation without secondary modulation. Three bands (f_0 = 923.6 MHz, B (signal bandwidth) = 0.2 MHz, f_0 = 2.432 GHz, B = 20 MHz, f_0 = 5.6 GHz, B = 20 or 200 MHz) signals are added to simulation input. We think we can demodulate any band, because we obtain all complex information for demodulation. We think that we can demodulate all bands. We select f_0 = 5.6 GHz signal for demodulation in this report. We select phase information at a center timing of acquisition data clock for demodulated data. Demodulation results for BPSK transmitted signals (B = 20 MHz, 63-bit m-sequence data) without noise using the proposed algorithm is shown in Fig. 15. We succeed to obtain demodulation data using low sampling frequency ADCs without IF and baseband filters. A demodulated data is shown in Fig. 16. Blue solid line is a demodulated data and red cross points are transmitted 63-bit data. Obtained data are coincident with the original data.

We add a white noise (several level) to transmitted signals as shown in Fig. 14. An obtained result for a relation between Bit-error rate and signal to noise ratio (S/N) for BPSK transmitted signals (fo = 5.6 GHz, B = 200 MHz, 1000-bit partial m-sequence data) using the proposed algorithm is shown in Fig. 17. Blue solid line is the theoretical curve for BPSK synchronous demodulation and red cross points are statistical results using this method. Obtained differences

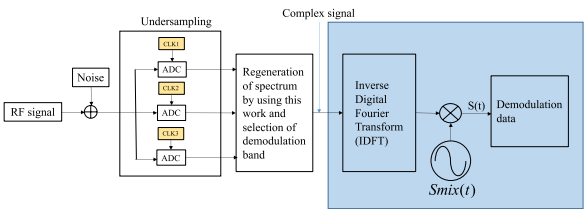

Fig. 14 Demodulation system using regenerated spectrum from undersampled signal by using proposed algorithm.

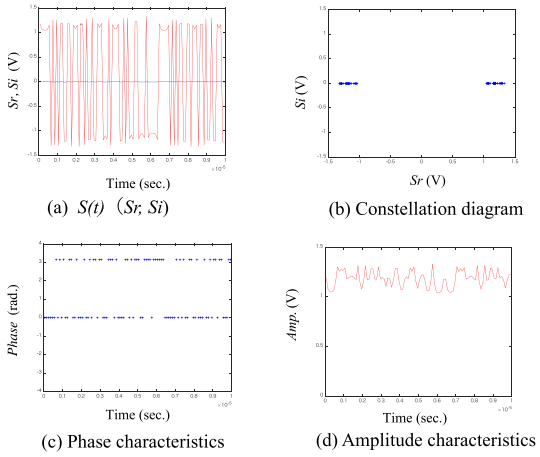

Fig. 15 Demodulation results for BPSK transmitted signals (B=20 MHz) using the proposed algorithm.

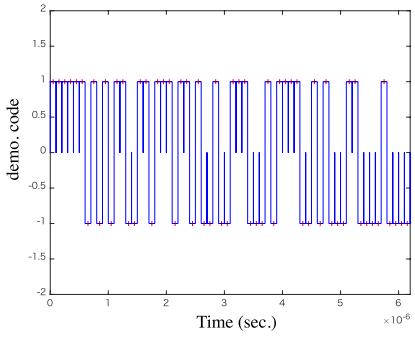

Fig. 16 Demodulation data for BPSK transmitted signals (B=20 MHz) using the proposed algorithm.

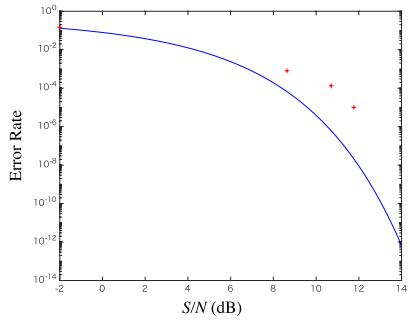

Fig. 17 Relation between Bit-error rate and signal to noise ratio (S/N) for BPSK transmitted signals (B=100 MHz) using the proposed algorithm.

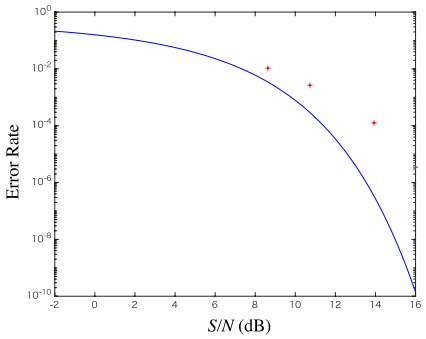

Fig. 18 Relation between Bit-error rate and signal to noise ratio (S/N) for QPSK transmitted signals (B=100 MHz) using the proposed algorithm.

from theoretical values are about 1.6 to 2.4 dB for S/N axis. We also apply this proposed algorithm to the QPSK modulation system. An obtained result for a relation between Bit-error rate and signal to noise ratio (S/N) for QPSK transmitted signals (fo = 5.6 GHz, B = 200 MHz, 2000-bit partial m-sequence data) using the proposed algorithm is shown in Fig. 18. Blue solid line is the theoretical curve for QPSK synchronous demodulation and red cross points are statistical results using this method. Obtained differences from theoretical values is about 1.3 to 2.9 dB for S/N axis. We consider that the demodulation method using this algorithm is succeeded.

6. Conclusion

We proposed a spectrum regeneration method for a direct undersampled real signal considering the spectrum folding direction, the complex conjugate relation and the convolution of even/odd spectrums at wrap frequency by using the extended algorithm. We showed the capability of the proposed spectrum regeneration method by using the simulation and the measured data. The availability of this proposed method is verified by the results. We also successfully obtained demodulated data from the regenerated spectrum.

Acknowledgments

This work includes results of the project entitled "R&D on Technologies to Densely and Efficiently Utilize Radio Resources of Unlicensed Bands in Dedicated Areas," and "R&D on Adaptive Media Access Control for Increasing the Capacity of Wireless IoT Devices in Factory Sites," which are supported by the Ministry of Internal Affairs and Communications as part of the research program "R&D for Expansion of Radio Wave Resources (JPJ000254)".

References

[1] Y. Han, Y. Chen, B. Wang, and K.J. Ray Liu, "Enabling heterogeneous connectivity in Internet of Things: A time-reversal approach," IEEE Internet Things J., vol.3, no.6, pp.1036–1047, March 2016.
[2] Q. Zhao and B.M. Sadler, "A survey of dynamic spectrum access," IEEE Signal Process. Mag., vol.24, no.3, pp.79–89, May 2007.
[3] T. Yücek and H. Arslan, "A survey of spectrum sensing algorithms for cognitive radio applications," IEEE Commun. Surveys Tuts., vol.11, no.1, pp.116–130, March 2009.
[4] M. Mishali, Y.C. Eldar, O. Dounaevsky, and E. Shoshan, "Xampling: Analog to digital at sub-Nyquist rates," IET Circuits Devices Syst., vol.5, no.1, pp.8–20, Jan. 2011.
[5] N.L. Tzou, D. Bhatta, and A. Chatterjee, "Low cost back end signal processing driven bandwidth interleaved signal acquisition using free running undersampling clocks and mixing signals," Proc. 2014 International Test Conference, pp.1–10, Oct. 2014
[6] S. Smaili and Y. Massoud, "Compressive sensing with sub-nyquist clocks using frequency division multiplexed random sequences," Proc. WAMICON 2012 IEEE Wireless & Microwave Technology Conference, April 2012.
[7] D. Arianandа and G. Leus, "Compressive wideband power spectrum estimation," IEEE Trans. Signal Process., vol.60, no.9, pp.4775–4789, Sept. 2012.
[8] G. Fudge, R. Bland, M. Chivers, S. Ravindran, J. Haupt, and P. Pace,"A nyquist folding analog-to-information receiver," Proc. Signals, Systems and Computers, 2008 42nd Asilomar Conference, pp.541–545, Nov. 2008.
[9] Y.K. Alp, G. Gok, and A.B. Korucu, "Sub-band equalization filter design for improving dynamic range performance of modulated wideband converter," Proc. 2017 25th European Signal Processing Conference (EUSIPCO), pp.917–921, 2017.
[10] W. Guo, Y. Kim, A.H. Tewfik, and N. Sun, "A fully passive compressive sensing SAR ADC for low-power wireless sensors," IEEE J. Solid-State Circuits, vol.52, no.8, pp.2154–2167, Aug. 2017.
[11] D. Cohen and Y.C. Eldar, "Sub-nyquist cyclostationary detection for cognitive radio," IEEE Trans, Signal Process., vol.65, no.11, pp.3004–3019, June 2017.
[12] Y. Zhao, Y.H. Hu, and J. Liu, "Random triggering-based sub-nyquist sampling system for sparse multiband signal," IEEE Trans. Instrum. Meas., vol.66, no.7, pp.1789–1797, July 2017.
[13] S.S. Ioushua, O. Yair, D. Cohen, and Y.C. Eldar,"CaSCADE: Compressed carrier and DOA estimation," IEEE Trans, Signal Process., vol.65, no.10, pp.2645–2658, May 2017.
[14] T. Xiong, H. Li, P. Qi, Z. Li, and S. Zheng, "Predecision for wideband spectrum sensing with sub-nyquist sampling," IEEE Trans. Veh. Technol., vol.66, no.8, pp.6908–6920, Aug. 2017.
[15] J. Gai, Y. Li, and K. Dong, "An implementation method of sub-nyquist sampling for spectrum-sparse signals," Proc. 2016 Sixth International Conference on Instrumentation & Measurement, Computer, Communication and Control, pp.898–903, 2016.
[16] A. Kwan, S.A. Bassam, and F.M. Ghannouchi, "Sub-sampling technique for spectrum sensing in cognitive radio systems," Proc. 2012 IEEE Radio and Wireless Symposium, pp.347–350, Jan. 2012.
[17] M. Mishali and Y.C. Eldar, "Blind multiband signal reconstruction: Compressed sensing for analog signals," IEEE Trans. Signal Process., vol.57, no.3, pp.993–1009, March 2009.
[18] R. Venkataramani and Y. Bresler, "Optimal sub-nyquist nonuniform sampling and reconstruction for multiband signals," IEEE Trans. Signal Process., vol.49, no.10, pp.2301–2313, Oct. 2001.
[19] M. Fleyer, A. Linden, M. Horowitz, and A. Rosenthal, "Multirate synchronous sampling of sparse multiband signals," IEEE Trans. Signal Process., vol.58, no.3, pp.1144–1156, March 2010.
[20] T. Moon, H.W. Choi, N. Tzou, and A. Chatterjee, "Wideband sparse signal acquisition with dual-rate time-interleaved undersampling hardware and multicoset signal reconstruction algorithms," IEEE Trans, Signal Process., vol.63, no.24, pp.6486–6497, Dec. 2015.
[21] H. Sun, W. Chiu, J. Jiang, A. Nallanathan, and H.V. Poor,"Wideband spectrum sensing with sub-nyquist sampling in cognitive radios," IEEE Trans. Signal Process., vol.60, no.11, pp.6068–6073, Nov. 2012.
[22] N. Wong and T. Ng, "An efficient algorithm for downconverting multiple bandpass signals using banclpass sampling," Proc. 2001 IEEE International Conference on Communications, pp.910–914, 2001.
[23] J. Zhang, T. Zhu, H. Zheng, Y. Kuang, M. Liu, and W. Huang,

"Breaking through the bandwidth barrier in distributed fiber vibration sensing by sub-Nyquist randomized sampling," Proc. 2017 25th Optical Fiber Sensors Conference (OFS), 2017.
[24] E. Astaiza1, P. Jojoa1, and F. Novillo, "Energy wideband spectrum sensing based on SubNyquist sampling and second order statistics," Proc. 2016 IEEE Ecuador Technical Chapters Meeting (ETCM), 2016.
[25] T. Furuichi, K. Akimoto, M. Motoyoshi, S. Kameda, and N. Suematsu, "A study on direct RF undersampling receiver configuration considering timing skew spurs using time-interleaved ADC," Proc. 2018 Asia-Pacific Microwave Conference (APMC), pp.1525–1527, Nov. 2018.
[26] S.K. Sharma, E. Lagunas, S. Chatzinotas, and B. Ottersten, "Application of compressive sensing in cognitive radio communications: A survey," IEEE Commun. Surveys Tuts., vol.18, no.3, pp.1838–1860, Feb. 2016.

Takashi Shiba received the B.S. and M.S. degrees in electronic engineering from Tohoku University, Sendai, in 1981 and the Ph.D. degree in communication engineering from Tohoku University, Sendai, in 2016. From 1981 to 2000, he was a Researcher and a Senior Researcher with Consumer Research Center in Hitachi Ltd. From 2000 to 2014, he was a Senior Engineer with Hitachi Media Electronics Co. Ltd. He researched and worked for Surface Acoustic Wave (SAW) devices, especially development of SAW devices for mobile-communication. From 2014 to 2019, he researched pulse type radars in the University of Electro-Communications. Since 2019, he has been Specially Appointed Professor with Research Institute of Electrical Communication in Tohoku University, Sendai. He has researched undersampling spectrum monitors for IOT systems in Tohoku University. He is the author of more than 50 articles, and more than 60 inventions. His research interests include SAW devices, SAW applications, signal processing of pulse MIMO radar and undersampling technologies.

Tomoyuki Furuichi received the B.S. degrees in electronics engineering from Nagaoka University of Technology, Japan, in 2017, and the M.S. degrees in communication engineering from Tohoku University, Japan, in 2019. He is currently working toward the Ph.D. degree in communication engineering. His current research interests are spectrum monitoring technologies for wireless IoT.

Mizuki Motoyoshi received the B.E. degree from the Sophia University Japan in 2005, M.E. and Ph.D. degree in Electronics Engineering from the University of Tokyo, Japan in 2007 and 2011, respectively. Since 2014, he has been assistant professor of the Research Institute of Electrical Communication, Tohoku University. He received the Young Researcher's Award in 2007 in IEICE. His research interests are on RFCMOS design and modeling for millimeter-wave wireless Communication.

Suguru Kameda received the B.S., M.S., and Ph.D. degrees in Electronics Engineering from Tohoku University, Sendai, Japan in 1997, 1999 and 2001, respectively. Since 2001, he has been with the Research Institute of Electrical Communication, Tohoku University, and is currently the Associate Professor. He is also a Visiting Scholar with WINLAB, Rutgers, the State University of New Jersey from September 2018 to March 2019, and an Invited Advisor with National Institute of Information and Communications Technology (NICT) from 2018. His current interests are in massive connect IoT, heterogeneous network, and satellite communication. Dr. Kameda received the TELECOM System Technology Award for Student in 2001, 2008 Young Investigator Award in Software Radio from IEICE Technical Committee on Software Radio, Best Paper Award of International Technical Conference on Circuits/Systems, Computers and Communications (ITC-CSCC 2012), 2014 Special Technical Award in Smart Radio from IEICE Technical Committee on Smart Radio, M. Ishida Foundation Research Award 2017 and Encouragement Award 2019 from the Miyagi Foundation for the Promotion of Industrial Science. He is a Member of the IEEE and the Japan Institute of Electronics Packaging (JIEP).

Noriharu Suematsu received the B.S., M.S. and Dr.Eng. degrees in Electronics and Communication Engineering from Waseda University in 1985, 1987 and 2000, respectively. From 1987 to 2010, he had been with Mitsubishi Electric, where he had been engaged in research and development of RF/microwave/millimeterwave semiconductor integrated circuits and transceivers for wireless communication and satellite communication. Since 2010, he has been a Professor of Research Institute of Electrical Communication (RIEC), Tohoku University. He received the Shinohara Award from the IEICE in 1991, the OHM Technology Award from the Promotion Foundation for Electrical Science and Engineering in 2002 and Prize for Science and Technology (Development Category) of the Commendation for Science and Technology by the Minister of Education, Culture, Sports, Science and Technology in 2009. He also received the Electronics Society Award from the IEICE in 2012. Currently, he is a director of Research Center for 21st Century Information Technology, RIEC, Tohoku University.